Appl Phys A (2010) 101: 411–416
DOI 10.1007/s00339-010-5834-6

Applied Physics A
Materials Science & Processing

Designs for optimizing depth of focus and spot size for UV laser ablation

An-Chi Wei · Jyh-Rou Sze · Jyh-Long Chern

Received: 23 November 2009 / Accepted: 10 May 2010 / Published online: 16 June 2010

Abstract The proposed optical systems are designed for extending the depths of foci (DOF) of UV lasers, which can be exploited in the laser-ablation technologies, such as laser machining and lithography. The designed systems are commonly constructed by an optical module that has at least one aspherical surface. Two configurations of optical module, lens-only and lens-reflector, are presented with the designs of 2-lens and 1-lens-1-reflector demonstrated by commercially optical software. Compared with conventional DOF-enhanced systems, which required the chromatic aberration lenses and the light sources with multiple wavelengths, the proposed designs are adapted to the single-wavelength systems, leading to more economical and efficient systems.

1 Introduction

Along with the development of the semiconductor technology and mechanic machining, various electronic and photonic devices have to be miniaturized. Either in semiconductor lithography or in laser machining, UV light is an important tool for ablation [1–5], owing to its short wavelength and the resultant high resolution [6]. Besides the resolution, the depth of focus (DOF) of UV light also affects the quality of the fabricated sample. However, in an optical system, it is usually a trade-off between high resolution and long DOF. Generally, when the resolution is enhanced, the DOF will be reduced, and then the qualities of longitudinal surfaces, such as the sharpness of the side wall and the surface roughness of the whole sample, will be liable to be degraded. Thus, how to generate a UV light source with high resolution and sufficient DOF is a significant task for further development of high-resolution fabrication technologies.

To extend the DOF of an optical system with a UV laser source, a lens with chromatic aberration was used to focus several narrow bands of radiation from an excimer laser [7]. Since each band was focused at a different focal plane, the overall foci did contribute to a long DOF. However, such an apparatus required a special light source with closely spaced and narrow bands. Hence, the uniformity of laser power along the optical axis is an issue and the expense of source would be high. Another method to extend DOF was demonstrated by applying diffractive optical elements (DOEs) [8]. Since DOEs are wavelength-sensitive elements, the DOEs for long-wavelength applications are fabricated by economical technologies; but for short-wavelength applications, the fabrication requires high-resolution technologies or complicated procedures. Meanwhile, if the number of levels of a DOE is not high enough, the efficiency will be reduced due to the diffraction of unnecessary orders. Thus, it is uneconomic to use DOEs for improving the DOF of UV light. To generate satisfactory DOF and resolution and to reduce the cost of the system, a single-wavelength aspherical optical module is proposed herein.

A.-C. Wei (✉)
Foxsemicon Integration Technology Inc., No. 16, Ke-jhong Rd., Jhu-nan Township, Miao-Li County, Taiwan, ROC
e-mail: an-chi.wei@foxsemicon.com

J.-R. Sze
Instrument Technology Research Center, National Applied Research Laboratories, No. 20, R&D Rd. VI, Hsinchu, Taiwan, ROC

J.-L. Chern
Department of Photonics, National Chiao Tung University, No. 1001, Ta-Hsueh Rd., Hsinchu, Taiwan, ROC

2 Theory

To evaluate the DOF and the resolution of an optical system, aberrations play an important role. For an aberrationless optical system, diffraction dominates the spot size and the DOF. The so-called diffractive depth of focus (DDOF) has a relationship with the f-number, F, [9]:

$$\mathrm{DDOF} = 16F^2 W_\mathrm{d}, \tag{1}$$

where W_d is the axial defocus. From (1), the acceptable W_d determines the DDOF when F of the system is fixed. According to Fourier optics, the axial intensity, as illustrated in Fig. 1, is a function of the wavelength λ and the axial defocus W_d:

$$I(0) = I_0\left[\frac{\sin(\frac{\pi W_\mathrm{d}}{\lambda})}{\frac{\pi W_\mathrm{d}}{\lambda}}\right]^2. \tag{2}$$

Then, one can refer to the intensity function to decide W_d. For example, if the required threshold intensity lies in the half of the maximum intensity, i.e. $I(0) = 0.5I_0$, W_d and DDOF can be calculated from (1) and (2) as $\lambda/2.26$ and $7.08\lambda F^2$, respectively. As for the resolution, based on the Rayleigh criteria [10], the minimal spot width at the focal plane is known as 2.44λF.

On the other hand, the DOF of a system with aberrations is determined by the blur spot, resulting from the light focusing short of the paraxial focal plane or beyond it [9]. Then the DOF can be counted from the geometry of the optical system, i.e. geometrical depth of focus (GDOF):

$$\mathrm{GDOF} \sim 2F W_\mathrm{B}, \tag{3}$$

where W_B is the acceptable width of the blur spot at the focal plane.

From (3), one can know that even though W_B is as good as the minimal spot width defined by Rayleigh criteria, GDOF ($\sim 4.88\lambda F^2$) is less than the DDOF of an aberrationless (diffraction-limit) system under the condition of threshold axial intensity lying in the half of the maximum intensity. Therefore, a DDOF-dominated system will have better performance than the GDOF-dominated system.

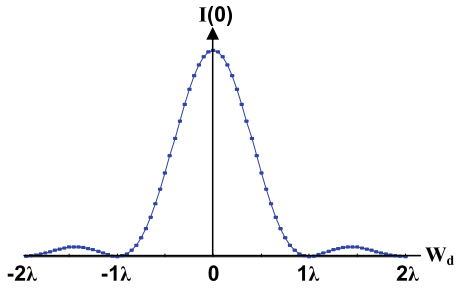

Fig. 1 Axial intensity distribution of an aberrationless optical system

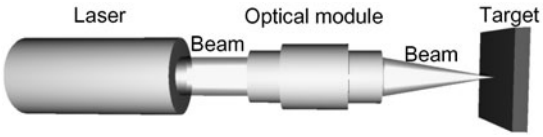

Fig. 2 Illustration of a system with a UV laser, an optical module and a target

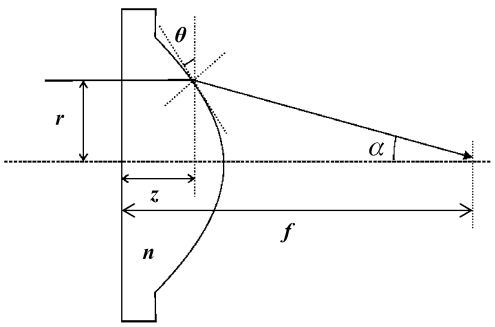

Fig. 3 Geometrical ray-tracing of a single-lens module to determine the lens profile

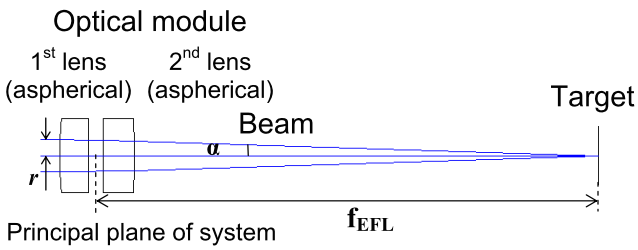

Fig. 4 Ray tracing of embodiment with one spherical lens and one aspherical lens

3 Design, and simulation results

The proposed systems are to acquire sufficient DOF and resolution for applications to UV lasers and collimated UV lights. Generally, one system is constructed by a single-wavelength UV light source, a target and an optical module consisting of a single, double or multiple optical components, as illustrated in Fig. 2. The characteristic of proposed optical module is that among the surfaces of the optical components, at least one surface has an aspherical profile to reduce aberrations. Since the required aspherical profile can be implemented by various configurations, lens–only and lens-reflector configurations are investigated as examples in this article.

Table 1 Parameters of the embodiment with one spherical lens and one aspherical lens

Surface	Radius[a] (mm)	Thickness[b] (mm)	Material[c]	Note
Beam-emergence	–	1.00×10^{20}	Air	–
The 1st surface of the 1st lens	117.717	10.000	Silica	–
The 2nd surface of the 1st lens	-1.018×10^3	5.033	Air	–
The 1st surface of the 2nd lens	-2.603×10^3	10.703	Silica	Aspherical
The 2nd surface of the 2nd lens	−307.307	159.800	Air	Aspherical

[a]Curvature radius

[b]Distance between current and next surfaces

[c]Material between current and next surfaces

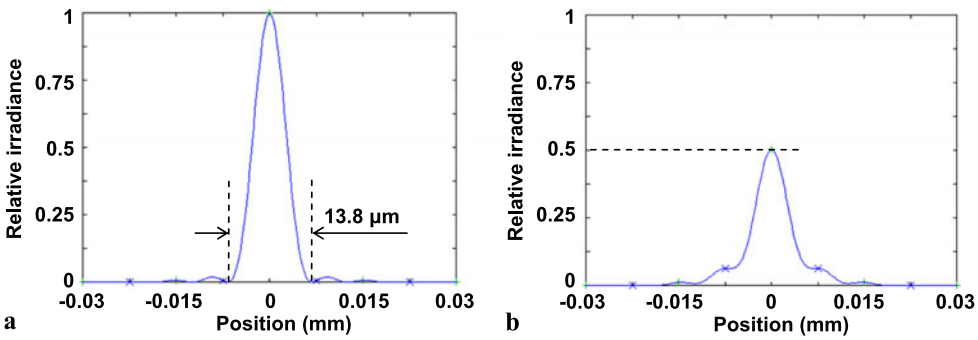

Fig. 5 Point-spread function of embodiment with one spherical lens and one aspherical lens (**a**) at the focal plane (**b**) at the plane 310 μm away from the focus

3.1 Lens-only configuration

For simplicity, a system with a single-lens module, as shown in Fig. 3, is considered. The first surface of the lens is assumed to be flat while the second one is an aspherical surface. Every differential segment of the second surface contributes to a certain focal length. Assume that the ith segment leads to a focal length f_i and its edge has a tilt angle of θ_i, a sag height of z_i and a radius of r_i. According to geometrical optics, θ_i is derived as:

$$\theta_i = \tan^{-1} \frac{\sin \alpha_i}{n - \cos \alpha_i}, \tag{4}$$

where α_i and n are the focal angle resulting from the ith segment and the refractive index of the lens, respectively. The focal angle α_i can be expressed as:

$$\alpha_i = \tan^{-1} \frac{r_i}{f_i - z_i}. \tag{5}$$

The focal length of the ith segment, f_i, shall be designed according to the uniformity of the focal spots along the optical axis; thus, it can be a function of its corresponding radius, i.e.:

$$f_i = f(r_i) \tag{6}$$

Substituting the initial conditions of the maximum radius R, its corresponding sag $Z_{\max}$ and the designed focal length function (6) into the (4) and (5) successively, one can derive the corresponding θ_i. Assume that the projection of every segment is a constant Δr, which means:

$$\Delta r = r_{i+1} - r_i. \tag{7}$$

From (7) the tilt angle θ_i can be also derived as:

$$\theta_i = \tan^{-1} \frac{z_{i+1} - z_i}{\Delta r}. \tag{8}$$

From (7) and (8), the successive r_{i+1} and z_{i+1} can be calculated. Reiterating the above steps, the profile of the lens will be obtained.

Because using double to multiple optical elements can divide the optical power with every element, resulting in an optical system more adaptive to the paraxial approximation, the optical performance, such as point-spread function (PSF) [11], will be better than that of the single-lens configuration. Therefore, the designed single-lens module can be decomposed to double or multiple lenses to acquire higher performance.

Numerical examples with two lenses, which have been simulated by OSLO, are described as follows. A UV laser with the wavelength of 355 nm and the beam diameter of 10.92 mm is applied as a light source. Assume that an optical system with $F = 15.93$ is used, and the threshold axial intensity lies in the half of the maximum intensity. Then,

the minimal spot width is 13.8 μm, and the DDOF counted from (1) is 638 μm. After optimization, a conventional system with two spherical lenses brings about a simulated DOF of 440 μm. When the proposed aspherical module is applied and optimized as a diffraction-limit system, the ray-tracing result is shown in Fig. 4 and the lens data are listed in Table 1. In Fig. 4, f_{EFL} represents the effective focal length of the system, while other parameters are the same as above definitions. The PSF at the focal plane and the plane where the peak intensity is attenuated to half maximum are simulated based on the diffraction beam propagation, as shown in Fig. 5(a) and (b), respectively. By simulating the PSF on the planes perpendicular to the optical axis, the plane with the peak intensity attenuated to the half maximum is found as 310 μm away from the focus in this example. From the results, the spot width at focus is ∼13.8 μm and the DOF is 620 μm, close to the theoretical results and superior to the conventional spherical lens module.

If a higher resolution is demanded, one spherical surface might not be enough to reach the requirement. One solution is to increase the number of aspherical surfaces. An example is given as follows. Assume that the wavelength and the beam diameter are as those in the above example. The required output spot size is 5 μm. The working distance of the double-lens module (60.19 mm in this example), the lenses thicknesses and the lens spacing are assumed to be fixed. Then, after optimization, a conventional module with double spherical lenses brings about a simulated DOF of 52 μm. When an optical module with two aspherical lenses is applied and optimized, the ray-tracing result is shown in Fig. 6 and the lens data are listed in Table 2. In Fig. 6, the definitions of parameters are the same as those in Fig. 4. The PSF at the focal plane and the plane where the peak intensity is attenuated to the half maximum (100 μm away from the focus in this example) are simulated, as shown in Fig. 7(a) and (b), respectively. The results show that the spot width at focus is ∼5 μm and the DOF is 200 μm, superior to the conventional spherical lens module. Noticeably, the relative

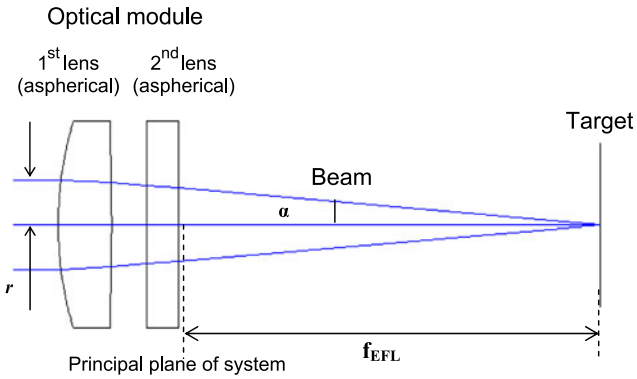

Fig. 6 Ray tracing of embodiment with two aspherical lenses

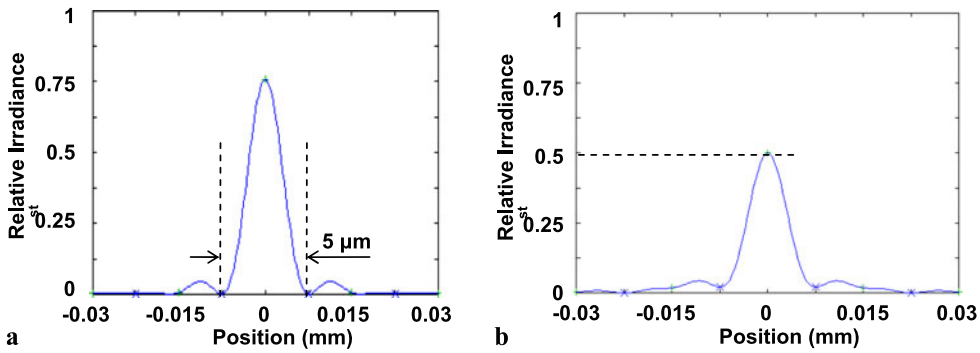

Fig. 7 Point-spread function of embodiment with two aspherical lenses (**a**) at the focal plane (**b**) at the plane 100 μm away from the focus

Table 2 Parameters of the embodiment with two aspherical lenses

Surface	Radius[a] (mm)	Thickness[b] (mm)	Material[c]	Note
Beam-emergence	–	1.00×10^{20}	Air	–
The 1st surface of the 1st lens	40.064	7.595	Silica	Aspherical
The 2nd surface of the 1st lens	−190.280	5.028	Air	Aspherical
The 1st surface of the 2nd lens	−18.538	4.497	Silica	Aspherical
The 2nd surface of the 2nd lens	0.239	60.190	Air	Aspherical

[a]Curvature radius

[b]Distance between current and next surfaces

[c]Material between current and next surfaces

irradiance of the designed system does not reach the unity, indicating an aberrated system. Then the simulated DOF is larger than the theoretical DDOF of 84 μm due to the aberration onto the sagittal plane.

3.2 Lens-reflector configuration

Besides lenses, the optical module can also include reflective elements such as ellipsoid or paraboloid mirrors. The advantage of using reflective elements lies in the shrinkage of the module length. Figure 8 is an example of two paraboloid mirrors arranged in a way of off-axis, followed by a focusing lens. Such a lens-reflector design can be further combined into one chip, which is known as planar integration of free-space optical components and is rather robust and compact [12].

Consider the configuration illustrated in Fig. 8. Assume the diameters of the incident and modulated beams are B and D, respectively. Then the magnification, m, is defined as D/B. According to the theory of planar beam expander [13], the focal lengths of the two paraboloid reflectors, f_a and f_b, have the relationships with the magnification and the distance between the apexes of the reflectors, d:

$$|f_a| + |f_b| = d, \tag{9}$$

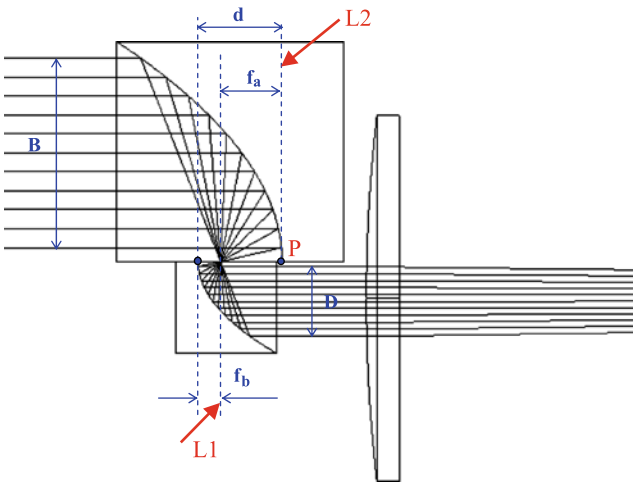

Fig. 8 Illustration of embodiment with lens and reflector

$$|f_b|/|f_a| = m. \tag{10}$$

Since the f-number is equivalent to the ratio of the effective focal length of the focusing element, f, to the modulated beam diameter, (10) can be rewritten as:

$$\frac{|f_b|}{|f_a|} = m = \frac{D}{B} = \frac{f}{FB}. \tag{11}$$

From (1) and (11), the focal lengths of the two paraboloid reflectors have the relationship with DDOF:

$$\frac{|f_b|}{|f_a|} = \frac{4f}{B}\sqrt{\frac{W_d}{\mathrm{DDOF}}}. \tag{12}$$

Consequently, using (9) and (12), one can derive the f_a and f_b for the two paraboloid reflectors.

A numerical example, which has been simulated by OSLO, is provided as follows. Assume the wavelength and the beam diameter are as those in above examples the distance between the apexes of the reflectors is: $d = 5$ mm, and the demanded DOF is 630 μm with the threshold axial intensity lying in the half of the maximum intensity. Then from (1) and (2), f-number can be counted as $F = 15.83$, while from the Rayleigh criteria, the minimal spot width at the focal plane is calculated as 13.7 μm. Consequently, applying (9) and (12), the focal lengths of the two reflectors are derived as: $|f_a| = 2.597$ mm and $|f_b| = 2.403$ mm. The third component is designated as a glass lens with the refractive index = 1.5, while other significant parameters are listed in Table 3. This design has been verified in simulation, as shown in Fig. 9. By means of the simulation of PSF, the plane where the peak intensity is attenuated to the half maximum is obtained as 338 μm away from the focus herein. From the results, the spot width at focal plane is ~13.8 μm and DOF is 676 μm, closing to the theoretical calculation and achieving the requirements. Compared with the first example with the double-lens module, this reflector-included design exhibits a shorter total track of module (reducing 15 mm) and a longer DOF under the same spot width at the focal plane.

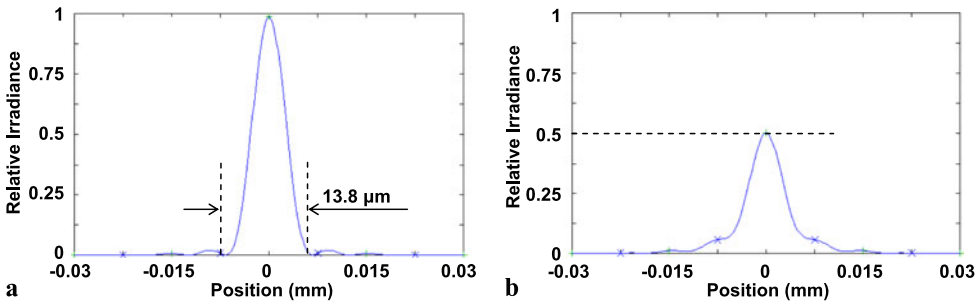

Fig. 9 Point-spread function of embodiment with two reflectors and one lens (**a**) at the focal plane (**b**) at the plane 338 μm away from the focus

Table 3 Parameters of the lens-reflector example

Surface	Radius[a] (mm)	Thickness[b] (mm)	Material[c]	Note
Beam-emergence	–	1.00×10^{20}	Air	–
The surface of the 1st reflector	−5.194	−5.000	Mirror	Paraboloid
The surface of the 2nd reflector	4.806	10.000	Mirror	Paraboloid
The 1st surface of the lens	80.000	1.000	Glass	$n = 1.5$
The 2nd surface of the lens	0	159.207	Air	–

[a]Curvature radius

[b]Distance between current and next surfaces; negative sign means reflection

[c]Material between current and next surfaces

4 Conclusions

Optical modules with aspherical components for extending the depths of foci (DOF) of UV lasers have been proposed. According to the theory of diffractive depth of focus, the lens-only and the lens-reflector configurations have been theoretically investigated, and their function of extending DOF has been demonstrated by simulations. From the simulated embodiments, the reflector-included aspherical module has presented the longer DOF with a more compact module size. Because of the advanced machining techniques, such as ultra-precision machining with diamond tools [14, 15], aspherical optics currently can be fabricated with the roughness beneath 0.01 μm and form error beneath 0.2 μm [14, 16]. Consequently, the proposed designs can be realized with the demanded performance. With proper designs, the proposed aspherical optical modules can be also applied to extend the DOF of the lasers with other wavelengths. Thus, various applications of the proposed modules shall be expected.

References

1. J. Prieur, F. Cau, J. Wais, A. Ostendorf, UV-laser machining offers new horizon in diffractive optical elements small-series manufacturing. Proc. SPIE **3099**, 69–73 (1997)
2. M. Reichling, J. Sils, H. Johansen, E. Matthias, Nanosecond UV laser damage and ablation from fluoride crystals polished by different techniques. Appl. Phys. A **69**, S743–S747 (1999)
3. M.C. Gower, Industrial applications of laser micromachining. Opt. Express **7**, 56–67 (2000)
4. T. Corboline, C.E. Rea, C. Dunsky, High power UV laser machining of Si wafers. Proc. SPIE **5063**, 495–500 (2003)
5. J. Amako, D. Sawaki, E. Fujii, High-efficiency diffractive beam splitters surface-structured on submicrometer scale using deep-UV interference lithography. Appl. Opt. **48**, 5105–5113 (2009)
6. E. Marom, N.A. Vainos, A.A. Friesem, J.W. Goodman, *Unconventional Optical Elements for Information Storage, Processing and Communications* (Springer, Berlin, 2000), pp. 247–255
7. U.S. Patent 5,303,002, 2004
8. Z. Liu, A. Flores, M.R. Wang, Diffractive infrared lens with extended depth of focus. Opt. Eng. **46**, 018002 (2007)
9. J.M. Geary, *Introduction to Lens Design: with Practical Zemax Examples*, Chap. 32 (Willmann-Bell, Richmond, 2002)
10. R.E. Fischer, B.T. Galeb, P.R. Yoder, *Optical System Design*, Chap. 4 (McGraw-Hill, New York, 2007)
11. J.W. Goodman, *Introduction to Fourier Optics*, Chap. 6 (McGraw-Hill, New York, 2005)
12. J. Jahns, A. Huang, Planar integration of free-space optical components. Appl. Opt. **28**, 1602 (1989)
13. A.C. Wei, H.P.D. Shieh, Design and analyses of a planar zoom module as a beam expander. Jpn. J. Appl. Phys. **43**, 5752 (2004)
14. E. Brinksmeier, R. Gläbem, J. Osmer, Ultra-precision diamond cutting of steel molds. CIRP Ann. Manuf. Technol. **55**, 551–554 (2006)
15. L. Li, A.Y. Yi, C. Huang, D.A. Grewell, A. Benatar, Y. Chen, Fabrication of diffractive optics by use of slow tool servo diamond turning process. Opt. Eng. **45**, 113401 (2006)
16. H.S. Kima, K.I. Lee, K.M. Lee, Y.B. Ban, Fabrication of free-form surfaces using a long-stroke fast tool servo and corrective figuring with on-machine measurement. Int. J. Mach. Tools Manuf. **49**, 991–997 (2009)